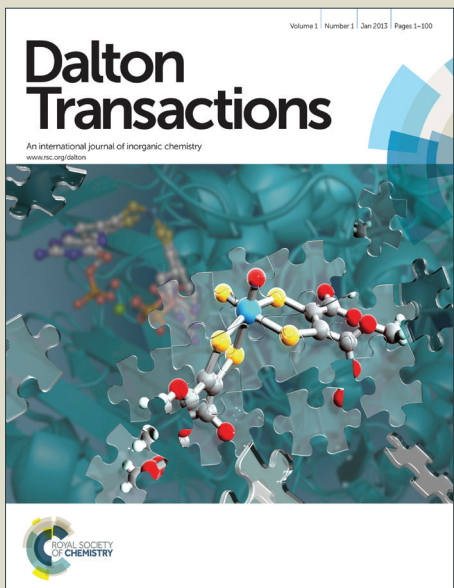


Dalton Transactions

Accepted Manuscript



This is an Accepted Manuscript, which has been through the Royal Society of Chemistry peer review process and has been accepted for publication.

Accepted Manuscripts are published online shortly after acceptance, before technical editing, formatting and proof reading. Using this free service, authors can make their results available to the community, in citable form, before we publish the edited article. We will replace this Accepted Manuscript with the edited and formatted Advance Article as soon as it is available.

You can find more information about Accepted Manuscripts in the [Information for Authors](#).

Please note that technical editing may introduce minor changes to the text and/or graphics, which may alter content. The journal's standard [Terms & Conditions](#) and the [Ethical guidelines](#) still apply. In no event shall the Royal Society of Chemistry be held responsible for any errors or omissions in this Accepted Manuscript or any consequences arising from the use of any information it contains.

Cite this: DOI: 10.1039/c0xx00000x

www.rsc.org/xxxxxx

ARTICLE TYPE**Supramolecular activation of a molecular photocatalyst**

Michael G. Pfeffer,^a Christian Pehlken^a, Robert Staehle^{a,b}, Dieter Sorsche^a, Carsten Streb^a and Sven Rau^{*a}

Received (in XXX, XXX) Xth XXXXXXXXX 20XX, Accepted Xth XXXXXXXXX 20XX

DOI: 10.1039/b000000x

The effects of the planar aromatic organic molecules anthracene and pyrene on the catalytic performance of the intramolecular hydrogen evolving photocatalyst $[\text{Ru}(\text{tbbpy})_2(\text{tpphz})\text{PdCl}_2](\text{PF}_6)_2$ functioning as photocatalytic dyad have been studied. $^1\text{H-NMR}$ studies on $[\text{Ru}(\text{tbbpy})_2(\text{tpphz})\text{PdCl}_2](\text{PF}_6)_2$ and $[\text{Ru}(\text{tbbpy})_2(\text{tpphz})](\text{PF}_6)_2$ show a pronounced interaction of pyrene with the ruthenium complexes due to π - π -interactions. The solid state structure of $[\text{Ru}(\text{tbbpy})_2(\text{tpphz})\text{PdCl}_2]_2[\text{Mo}_8\text{O}_{24}]$ shows a pronounced π -stacking of the polycyclic ligands. In addition, dimerization constants for the complexes and association constants between the complexes and pyrene were determined. Studies into the photocatalytic hydrogen production show a decreased induction phase and increased turn over frequencies during the initial phase of the catalysis in the presence of anthracene and pyrene utilising the catalyst $[\text{Ru}(\text{tbbpy})_2(\text{tpphz})\text{PdCl}_2](\text{PF}_6)_2$ irrespective of the nature of the polycyclic aromatic hydrocarbon.

Introduction

Photocatalytic dyads based on hetero-oligonuclear complexes, i.e. intramolecular photocatalysis are an intriguing development at the interface between molecular catalysis, photochemistry and energy science. The ability to combine molecular building blocks carrying specific functions into large functional units is a prerequisite for this area. This general concept has been termed photochemical molecular devices, PMD.¹ In order to generate photocatalytically active PMDs the following functionalities are required: visible light absorption, generation of reactive, long lived charge separated states, directional electron transfer between catalytic site and photocentre and catalytic transformation of the substrate at the catalytic site. Recent examples of intramolecular photocatalysts include water oxidation catalysts, water reduction catalysts and carbon dioxide reducing examples.²⁻¹¹ In direct comparison with intermolecular¹²⁻¹⁶ and heterogeneous photocatalysts¹⁷⁻²⁰ intramolecular photocatalysis, however, often suffer from lower catalytic activity. It is therefore of paramount importance to learn more about the factors determining the catalytic activity of intramolecular photocatalysts. Towards this aim two main routes may be envisaged: i) the synthesis of new catalysts^{21,22}; ii) the optimization of existing catalytic systems by supplying activating additives. As it is currently not fully clear which design criteria have to be taken into consideration for the *de novo* synthesis of active catalysts, route ii) deserves further attention. Route ii) can be taken by screening properties of the catalytic system like solvent composition, pH value and ionic additives.^{5,7,23-27} Within this research it has for instance been shown that the addition of $\text{N}(\text{C}_4\text{H}_9)_4\text{Cl}$ to the photocatalytic system for the light induced formation of hydrogen from water based on

$[\text{Ru}(\text{tbbpy})_2(\text{tpphz})\text{PdCl}_2](\text{PF}_6)_2$ (**RutpphzPd**) (Ruthenium(II)-bis(4,4'-di-tert-butyl-2,2'-bipyridyl)-(μ-tetrapyrrido[3,2-*a*:2',3'-*c*:3'',2'',-*h*:2'',3'',-*j*]phenazine)-(dichloropalladium)-dihexafluorophosphate) (Fig. 1) leads to a significant drop in catalytic activity. This has been explained by the inhibition of a chloride ligand loss from the catalytic centre, a process crucial for catalytic turnover.⁷ Furthermore, the photocatalytic activity of this system can be increased by addition of appropriate amounts of water^{21,22,28} and completely inhibited by changing the solvent to dichloromethane.⁷ Since the photocatalytic activity of this molecular systems is dependent on the interplay between photochemical electron transfer and catalytic steps in combination with the molecular building blocks all occurring within the molecular architecture, a careful analysis of these steps should provide new starting points for the investigation of new activating additives. Starting point is the structural analysis, which shows that **RutpphzPd** features a planar polycyclic tetrapyridophenazine bridging ligand. The mononuclear parent ruthenium complex $[\text{Ru}(\text{tbbpy})_2(\text{tpphz})](\text{PF}_6)_2$ **Rutpphz** (Fig.1) exhibits significant π - π -interactions in the solid state and a concentration dependent $^1\text{H-NMR}$ spectrum is observed.⁷ The planar ligand structure has previously been utilized for detailed dimerization studies of the related mononuclear ruthenium complex $[\text{Ru}(\text{bpy})_2(\text{tpphz})](\text{PF}_6)_2$ in solution.²⁹⁻³³ More recently DNA intercalation of tpphz-based Ru complexes has been utilized to access reversible luminescent switches.^{34,35} Here, we present a concise route, which allows optimization of the photocatalytic activity of **RutpphzPd** by controlling the supramolecular aggregation in solution. The concept uses polycyclic aromatic hydrocarbons to form π - π -interactions with the planar tpphz ligand, resulting in a dis-assembly of the π -stacked catalyst aggregates in solution.

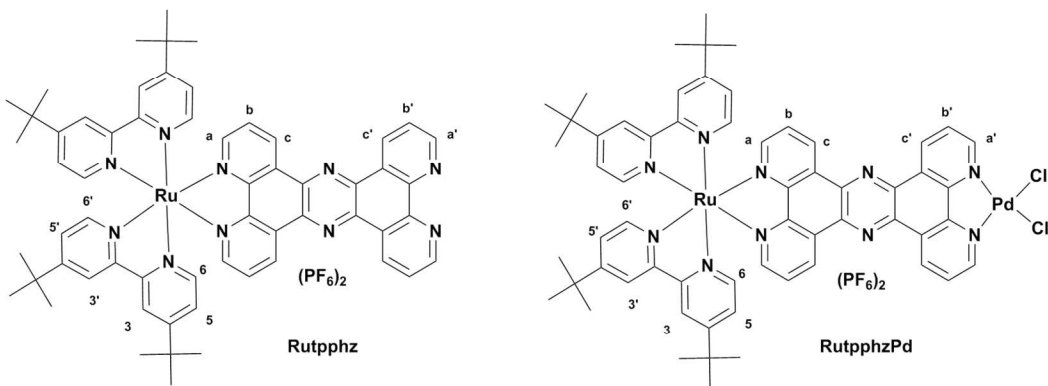


Fig. 1 Structure of the ruthenium complexes and assignments of the ligand protons.

Experimental

Starting materials

Anthracene (Anth) and pyrene (Pyr) were purchased from commercial sources and used without further purification. ¹⁰ [Ru(tbbpy)₂(tpphz)][PF₆]₂ (**Rutpphz**) and [Ru(tbbpy)₂(tpphz)PdCl₂](PF₆)₂ (**RutpphzPd**) were prepared according to literature methods.³⁶ All solvents used for the photocatalytic experiments were degassed with argon.

15 Crystal structure determination

Crystals of [(tbbpy)₂Ru(tpphz)Pd(Cl)]₂[Mo₈O₂₆]·ca. 18 DMF·2 H₂O suitable for X-ray diffraction crystallography were obtained by diffusion of a DMF solution of [Ru(tbbpy)₂(tpphz)PdCl₂](PF₆)₂ into a DMF solution of ²⁰ (TBA)[Mo₆O₁₉] (TBA = tetrabutylammonium) at 8 °C.

The crystal was mounted onto a MicroLoop™ using Fomblin oil. X-ray diffraction intensity data were measured at 180 K on a Agilent Technologies SuperNova single-crystal X-ray diffractometer using MoK α radiation. The structure was solved ²⁵ by direct methods (SHELXS) and refined by full-matrix least squares techniques against F_o^2 (SHELXL-2013).³⁷ During the refinement, significant disorder of the solvent DMF molecules in the crystal lattice was observed. Three DMF molecules and one oxygen atom corresponding to water were refined anisotropically, ³⁰ three DMF molecules were refined isotropically with fixed coordinates. For the remaining solvent accessible voids within the lattice, the Platon Squeeze procedure was applied to remove diffuse electron density. Based on the accessible void space, the amount of DMF within the voids was estimated to eight DMF ³⁵ molecules.^{38,39} It is noteworthy that according to the obtained data, the ion lattice of the ruthenium/palladium complex and the molybdate cluster only accounts for approximately 50% of the crystal volume.

The hydrogen atoms were included at calculated positions with ⁴⁰ fixed thermal parameters. All non-hydrogen atoms of the molybdate cluster and the RuPd complex were refined

anisotropically.

Crystal data for [(tbbpy)₂Ru(tpphz)Pd(Cl)]₂[Mo₈O₂₆]·ca. 18 DMF·2H₂O: C₁₆₈H₂₃₂Cl₄Mo₈N₃₈O₄₄Pd₂Ru₂, M_r = 4812.16 g mol⁻¹, orange block, crystal size 0.1336 x 0.067 x 0.0623 mm³, triclinic, space group P-1, a = 14.6799(3), b = 19.1828(4), c = 22.7309(5) Å, α = 103.457(2)°, β = 106.027(2), γ = 104.881(2), V = 5619.3(2) Å³, T = 180 K, Z = 1, $\rho_{\text{calcd.}}$ = 1.422 g cm⁻³, μ (Mo-K α) = 0.836 mm⁻¹, F(000) = 2442, altogether 72507 independent reflexes up to h(-18/18), k(-23/23), l(-28/28) measured in the range of 3.4° ≤ Θ ≤ 26.372°, completeness Θ_{max} = 99.7 %, 22937 unique reflections, R_{int} = 0.046, 22937 reflections with F_o > 4 σ(F_o), 1007 parameters, 18 restraints, R₁_{obs} = 0.0447, wR₂_{obs} = 0.1337, R₁_{all} = 0.0744, wR₂_{all} = 0.1442, 55 GOOF = 0.705, largest difference peak and hole: 0.990 / -0.546 e/Å⁻³. CCDC 987314 contains the supplementary crystallographic data for this paper. These data can be obtained free of charge from The Cambridge Crystallographic Data Centre via www.ccdc.cam.ac.uk/data_request/cif.

60 Instrumentation

¹H (400.13 MHz) spectra were measured with a Bruker DRX 400 spectrometer. The NMR spectra were recorded in acetonitrile-d₆ at 298 K. NMR chemical shifts were referenced to the solvent peak for acetonitrile (δ = 1.94 ppm).

⁶⁵ MS analysis was performed on a Shimadzu LC-MS 2020 equipped with an electrospray ionisation source and a SPD-20A UV/Vis detector.

The hydrogen evolved was measured by headspace gas chromatography (GC) on a Bruker Scion GC/MS, with a thermal ⁷⁰ conductivity detector (column: Mol. Sieve 5A 75m x 0.53 mm I.D., oven temp. 70 °C, flow rate 22.5 ml/min, detector temp. 200 °C) with argon as carrier gas. The GC was calibrated by mixing different volumes of pure hydrogen together with argon into a schlenk vessel. The obtained signal was plotted against the ⁷⁵ calibration curve and multiplied accordingly to receive the total produced hydrogen content in the headspace.

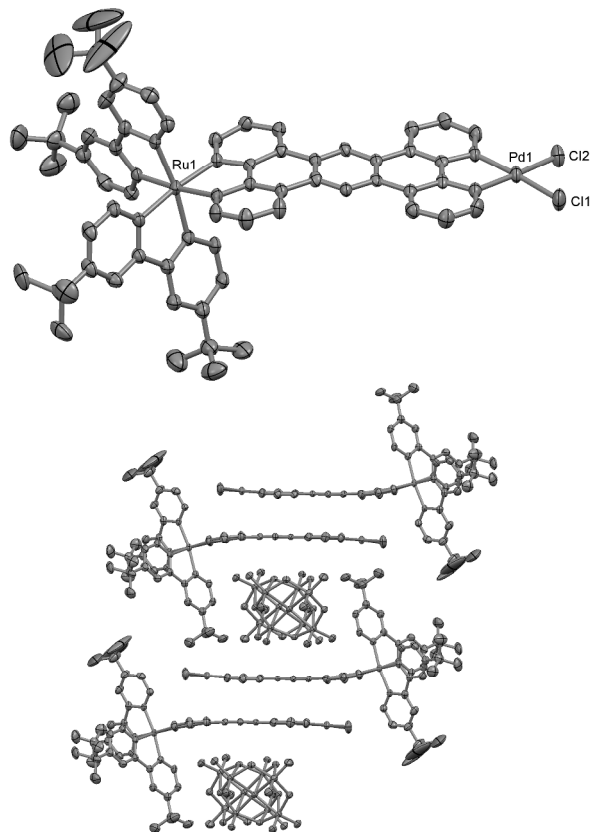
The UV/vis-spectra were recorded with a JASCO Spectrometer V-670. Quartz cells with a 10 mm path length were used.

The emission spectra were recorded with a JASCO ⁸⁰ Spectrofluorometer FP-8500. Quartz cells with a 10 mm path

length were used. All experiments were repeated 3 times. If not mentioned otherwise all experiments were performed under aerobic conditions.

5 Experimental conditions for photocatalytic hydrogen generation

Photohydrogen production experiments were carried out using a custom-made LED-based irradiation setup, which allowed irradiation at constant temperature (see Supp. Info. Fig. S1). The 10 acetonitrile used was freshly distilled under argon. The samples for the LED light irradiation experiments were prepared in GC vials (diameter = 45 x 14.75 mm) with a known headspace of 3 ml and a headspace-solution ratio of 3/2. Furthermore the GC vials were charged in the dark and under argon stream. After 15 addition of triethylamine ($V = 0.6$ ml) and 10 vol-% of degassed water ($V = 0.20$ ml) the final catalyst concentration in acetonitrile was 70 μM . Subsequently, the GC vials were irradiated with blue LED light (470 nm, $P = 30 - 40$ mW). In the case of the addition of anthracene or pyrene, 0.7 μmol (5-fold), 11.2 μmol (80-fold) 20 or 16.8 μmol (120-fold excess to the photocatalyst **RutpphzPd**) of the aromatic compound were added to the catalytic mixture as a solid. All samples were sonicated for 5 min to fully dissolve the polyaromatics. After irradiation, 200 μl samples were taken from the headspace and instantly analyzed by GC-MS. Irradiation 25 experiments and hydrogen measurements were repeated several times.



55

$^1\text{H-NMR}$ dimerization and association experiments

Typically, a concentrated stock solution of the complexes (ca. 10 30 mM) and the aromatic compound (ca. 20 mM) were prepared and the samples were allowed to equilibrate for several minutes. The dimerization constants and the association constant were calculated on the basis of the change of the chemical shift of selected protons following literature methods.^{42,43,45}

35 Results and Discussion

Supramolecular interactions of the Ru-complexes

Supramolecular π - π -interactions between the aromatic tpnaz ligands of **Rutpphz** in the solid state are well known.⁷ For this reason, we also investigated the solid-state structure of 40 $[\text{Ru}(\text{tbbpy})_2(\text{tpnaz})\text{PdCl}_2](\text{PF}_6)_2$ (**RutpphzPd**) with single crystal X-Ray diffractometry. Crystallization was facilitated by addition of a large polyanionic metal oxide cluster. The anion, $[\text{Mo}_8\text{O}_{24}]^{4-}$ was formed *in situ* by a known re-arrangement reaction starting from $(\text{TBA})_2[\text{Mo}_6\text{O}_{19}]$,⁴⁰ giving the complex salt 45 $[\text{Ru}(\text{tbbpy})_2(\text{tpnaz})\text{PdCl}_2]_2[\text{Mo}_8\text{O}_{24}]$ ca.18 DMF·2 H₂O (Fig. 2). As expected, an octahedral coordination is observed for the ruthenium (II) centre; the palladium (II) centre shows square-planar coordination mode. All distances and angles are in the expected range.^{7,41} However, it is obvious that the tpnaz ligand 50 deviates significantly from planarity and is also not coplanar with the equatorial plane of the ruthenium(II) coordination polyhedron, see Fig. 2.

Fig. 2 Top: X-ray crystal structure of the complex cation $[\text{Ru}(\text{tbbpy})_2(\text{tpnaz})\text{PdCl}_2]^{2+}$ (top; ellipsoids at 50% probability; counter 60 ions, solvent molecules and hydrogen atoms were omitted for clarity) in the solid state. Bottom: Stacking motive of four Ru-complexes and two molybdate clusters in the solid state.

The Ru-complex forms a cavity in which the anionic metal cluster is embedded. The distance between the mean planes of the tpnaz ligands of two **RutpphzPd** complexes (3.309 Å) is marginally smaller than for the mononuclear complex **Rutpphz** (3.397 Å), which shows that π - π -interactions are a crucial aspect for understanding this supramolecular photocatalyst.

70 Identification of Rutpphz and RutpphzPd by $^1\text{H-NMR}$ spectroscopy

As expected, $^1\text{H-NMR}$ studies revealed a concentration dependency of the chemical shifts of **Rutpphz** and **RutpphzPd**, which is due to π -stacking interactions between the planar tpnaz ligands (see Supp. Info. Fig. S10 and S12). In order to take this concentration dependency into account and due to the fact that both complexes show the identical $^1\text{H-NMR}$ signal types (Fig. 3), the identification value I was introduced, to facilitate the identification of both species, **Rutpphz** and **RutpphzPd**. For this 80 purpose several samples of each complex with defined concentration were prepared and allowed to equilibrate. From the $^1\text{H-NMR}$ spectra, the identification values I were calculated, based on the chemical shifts of protons H^c, H^{c'}, H^a and H^b (Table S3), where H^c, H^{c'} and H^a belong to the tpnaz ligand. H^b belongs

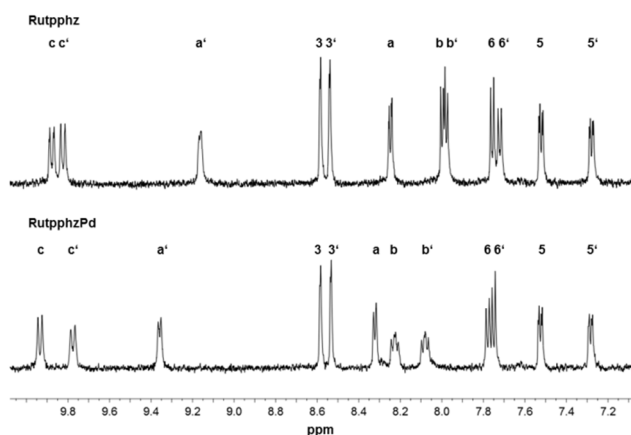


Fig. 3 ^1H -NMR spectra of **Rutpphz** and **RutpphzPd** at a concentration of 1 mM in acetonitrile-d₃

to the coordinated bipyridine, which is only marginally affected by the π - π -interaction.^{29–33} Therefore a simple equation was established empirically to convert the particular chemical shift values of protons H^c, H^{c'}, H^{a'} and H⁶ into a specific identification value *I* for each complex (Equation 1).

$$I = (\delta \text{H}^c - \delta \text{H}^6) \cdot (\delta \text{H}^{c'} - \delta \text{H}^{a'}) \quad (1)$$

The difference between the chemical shift values of H^c and H⁶, ($\delta \text{H}^c - \delta \text{H}^6$), is decreasing, whereas the difference of the chemical shift values between H^{c'} and H^{a'}, ($\delta \text{H}^{c'} - \delta \text{H}^{a'}$), is increasing in the same order with a rising complex concentration. The product of both terms delivers a constant value, which is specific for each compound. Within a concentration range of 0.25 mM to 10 mM stable values for *I* (**Rutpphz**) = 1.42 ± 0.04 and *I* (**RutpphzPd**) = 0.89 ± 0.04 were obtained. These specific identification values allow for unambiguous identification of **Rutpphz** and **RutpphzPd** independent from the concentration of the complex. This procedure was applied throughout the presented investigations for ensuring the purity of the two complexes under scrutinization.

25 Determination of the dimerization constants for Rutpphz and RutpphzPd

The π - π dimerization constant K_{π-D} was determined in acetonitrile according to the method used by Dixon and Lezna.^{42,43} Therefore the magnitude of the shift of the ^1H -NMR signals of the tpphz protons H^{a'} and H^{c'} due to dimerization were analyzed. K_{π-D} was calculated from the extrapolation of the δ values of H^{a'} and H^{c'} of free monomers δ_0 and fully stacked species δ_s as previously reported (see Supp. Info. Fig. S11).⁴² Table 1 shows the calculated values for K_{π-D}(**Rutpphz**):

Table 1 Calculated K_{π-D}(**Rutpphz**) values for the tpphz protons H^{a'} and H^{c'} and the average value.

K _{π-D} H ^{c'}	K _{π-D} (av)	K _{π-D} H ^{a'}
$113 \pm 10 \text{ M}^{-1}$		$131 \pm 10 \text{ M}^{-1}$
	$122 \pm 19 \text{ M}^{-1}$	

Kol and coworkers determined this constant for [Ru(bpy)₂(tpphz)](PF₆)₂ in acetonitrile and calculated K_{π-D} (av) = $185 \pm 75 \text{ M}^{-1}$.²⁹ These values are slightly different which may be explained with the slight chemical differences between both tpphz complexes. It was not possible to determine this constant for **RutpphzPd**, as the precision of the extrapolation for δ_0 in that concentration range was too low, due to the detection limit of the ^1H -NMR analysis. Nevertheless, comparison of the change of the ^1H -NMR signals of H^c, H^{a'} and H^{c'} of **Rutpphz** and **RutpphzPd** indicates two trends (Table 2). On the one hand, the signal of H^c of **RutpphzPd** is not influenced by dimerization in contrast to H^c of **Rutpphz**. This is plausible as the degree of overlap of two **RutpphzPd** complexes is altered, due to the steric influence of the PdCl₂ moiety as seen in Figure 2. On the other hand, the extent of the peak shift of the protons H^{a'} and H^{c'} is much larger for **Rutpphz** than for **RutpphzPd** indicating a larger π - π dimerization constant for **Rutpphz**.

Table 2 ^1H -NMR concentration dependency of **Rutpphz** and **RutpphzPd** in acetonitrile-d₃ with regard to the chemical shifts of protons H^c, H^{c'} and H^{a'}.

[mM]	Rutpphz			RutpphzPd		
	c	δH^c [ppm]	$\delta \text{H}^{c'}$ [ppm]	$\delta \text{H}^{a'}$ [ppm]	δH^c [ppm]	$\delta \text{H}^{c'}$ [ppm]
10	9.54	9.30	8.36	9.89	9.49	9.05
5.0	9.65	9.47	8.62	9.92	9.57	9.14
1.0	9.82	9.75	9.07	9.91	9.69	9.27
0.50	9.89	9.86	9.23	9.91	9.79	9.38
0.25	9.92	9.90	9.29	9.91	9.91	9.49

60 Interactions between anthracene and pyrene with RutpphzPd

Due to the π - π -interaction between the planar tpphz ligands of **Rutpphz** and **RutpphzPd** a possible interaction of such complexes with other planar aromatic molecules seemed interesting. Anthracene (anth) and pyrene (Pyr) were chosen for this study as model compounds. The interaction between the complexes and the two aromatics was monitored via ESI-mass spectrometry, ^1H -NMR and UV-vis spectroscopy. In addition, association constants were determined to analyze the extent of the interaction.

The mass spectrometry gave first hints for the formation of **RutpphzPd**-Anth/Pyr adducts. The analysis of the spectral data of an acetonitrile solution of **RutpphzPd** with anthracene showed a signal at m/z = 600 (z = 2) corresponding to the divalent cationic adduct between **Rutpphz** and anthracene. Identical investigations of **RutpphzPd** and pyrene resulted in the observation of the corresponding **Rutpphz**-Pyr adduct at m/z = 758 (z = 2). The loss of the palladium dichloride moiety readily occurs under ESI-MS conditions.²²

In the case of anthracene as interacting agent no association constant could be determined, since a fast photocatalytically induced dimerization of anthracene was competing with the intended supramolecular interaction and thus, concentration depended ^1H -NMR investigations were difficult to accomplish. A similar photocatalytic effect was observed by Castellano et al. with [Ru(dmb)₃]²⁺ (dmb = 4,4'-dimethyl-2,2'-bipyridine) as light absorber, which sensitizes the dimerization of anthracene by visible light.⁴⁴

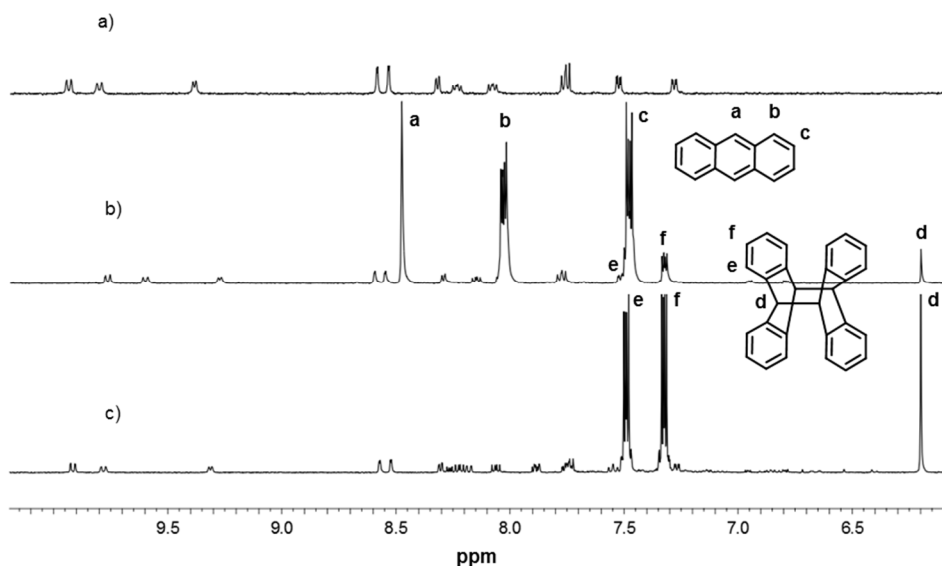


Fig. 4 Changes in the ^1H -NMR spectrum of **RutpphzPd** with anthracene after visible light irradiation: (a) ^1H -NMR spectrum of **RutpphzPd** ($c = 1 \text{ mM}$) in acetonitrile- d_3 ; (b) ^1H -NMR spectrum after the addition of anthracene ($c = 10 \text{ mM}$) and short exposure to ambient light. (c) ^1H -NMR spectrum after 60 min of irradiation with LED light (470 nm, 30 - 40 mW).

5

This has been explained by a triplet-triplet energy transfer from the ruthenium chromophor to anthracene and a subsequent dimerization. Similar to these literature results, our ^1H -NMR spectroscopic investigations on a sample containing **RutpphzPd** and anthracene in acetonitrile showed, already with ambient light irradiation, a formation of the anthracene dimer (Fig. 4). The effect becomes more pronounced after 60 minutes of LED irradiation (470 nm) leading to a complete dimer formation as evident from the ^1H -NMR data in Figure 4. Similar results were observed for **Rutpphz** (see Supp. Info. Fig. S5).

As illustrated in Figure 5, the dimerization of anthracene could also be observed via UV-vis spectroscopy in terms of a decreasing concentration of the anthracene monomer. After 120 minutes of LED (470 nm) irradiation, the absorption intensity of the monomer is significantly reduced, however the decrease is

less pronounced compared to the ^1H -NMR investigations, since much lower concentrations of anthracene were used due to technical requirements.

In contrast to anthracene, the interaction between **RutpphzPd** and pyrene can be analyzed via ^1H -NMR spectroscopy because pyrene shows no dimerization or other changes due to irradiation. Here, as expected, one can observe a pronounced influence of pyrene on the ^1H -NMR spectroscopical data of the ruthenium complex (Fig. 6). To evaluate the type of interaction the method of continuous variation (Job's method) for ^1H -NMR data was used⁴⁵ which suggested a 1/1 stoichiometry for the **RutpphzPd**-Pyr adduct (see Supp. Info. Fig. S7).

After the determination of the stoichiometry the association constant was calculated using a non linear global curve fitting treatment^{45,46} of concentration dependent ^1H -NMR spectroscopic data of **RutpphzPd** and pyrene which resulted in an association constant of $K_a = 155 \pm 44 \text{ M}^{-1}$ (see Supp. Info. Fig. S8).

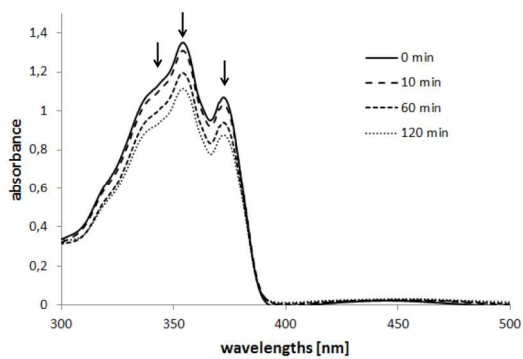


Fig. 5 Changes in the absorption spectrum of anthracene with **RutpphzPd** in acetonitrile ($c(\text{anthracene}) = 0.28 \text{ mM}$, $c(\text{RutpphzPd}) = 3.5 \mu\text{M}$, v% ($\text{H}_2\text{O}) = 0.5 \%$) with continuous LED light irradiation (470 nm).

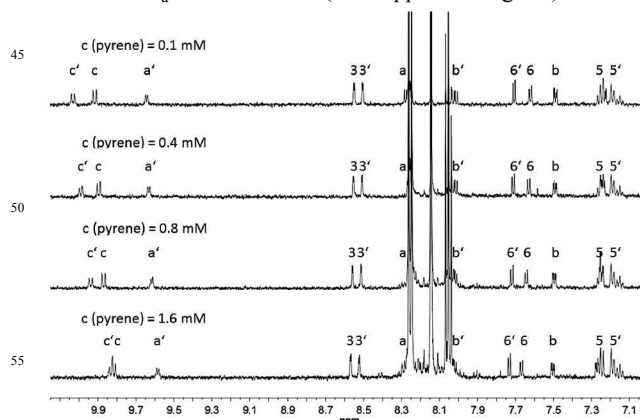
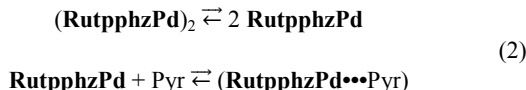


Fig. 6 Excerpt of ^1H -NMR dependency of the chemical shifts of **RutpphzPd** ($c = 0.1 \text{ mM}$) on the concentration of pyrene in acetonitrile- d_3 .

60

Photocatalysis

As the chemical environment of **RutpphzPd** is significantly altered by the addition of pyrene (Pyr) and a 1/1 adduct is formed, investigations into the effect of pyrene and the related anthracene on photocatalytic hydrogen evolution were performed. The formation of the 1/1 adduct is to compete with the dimerization of the complex (Equation 2).



In fact the dimerization should only play a minimal role during photocatalysis, as the dimerization constant of **Rutpphz** is relatively small and the concentration dependent shift of the proton signals of **RutpphzPd** is less pronounced as for **Rutpphz**. Therefore the amount of dimerized complexes within the concentration range of the catalytic mixtures should only be marginal.

During the experiments, 5-fold, 80-fold and 120-fold* molar excess of pyrene with respect to the complex concentration was added to a catalytic mixture of the following composition: $c(RutpphzPd) = 70 \mu\text{M}$, $V(\text{TEA}) = 0.6 \text{ mL}$ (2.2 M), $V(\text{ACN}) = 1.2 \text{ mL}$, $V(\text{H}_2\text{O}) = 0.2 \text{ mL}$. Due to the obtained **RutpphzPd**-Pyr association constant maximal equilibrium concentrations of $c(RutpphzPd\text{-Pyr})$ can be estimated for the pyrene containing system (Table 3). Thus about one in twenty catalyst molecules interact with pyrene for a 5-fold excess and about every second molecule for an 80-fold and 120-fold excess.

Table 3 Potential equilibrium concentration of the **RutpphzPd**-Pyr adduct in the catalytic mixture; $K_a = 155 \text{ M}^{-1}$, $[RutpphzPd]_0 = 70 \mu\text{mol}$.

excess pyrene	$[\text{Pyr}]_0$	$[\text{RutpphzPd-Pyr}]$	degree of association $[\text{RutpphzPd-Pyr}]/[\text{RutpphzPd}]_0$
5-fold	350 μmol	3.6 μmol	5.1 %
80-fold	5600 μmol	32.4 μmol	46.3 %
120-fold*	8400 μmol	39.5 μmol	56.4 %

* represents maximal concentration obtainable due to solubility

In addition a catalytic mixture with a 80-fold excess of anthracene was investigated. As this combination performs in the absence of the electron donor TEA photocatalytic dimerization of anthracene we were curious whether this photocatalytic process inhibits the photocatalytic hydrogen production. To investigate the effect of the supramolecular interactions on the kinetics of the photocatalytic hydrogen production, the samples containing the photocatalyst in combination with either anthracene or pyrene were compared to samples containing only the photocatalyst. All probes were prepared and kept under oxygen free atmosphere and irradiated with LED light (470 nm) of the same intensity. After a specific irradiation time the amount of produced hydrogen was determined via headspace GC.

It is apparent that the addition of a 80-fold excess of anthracene or pyrene leads to a significant acceleration of the photocatalytic hydrogen production (Fig. 7).

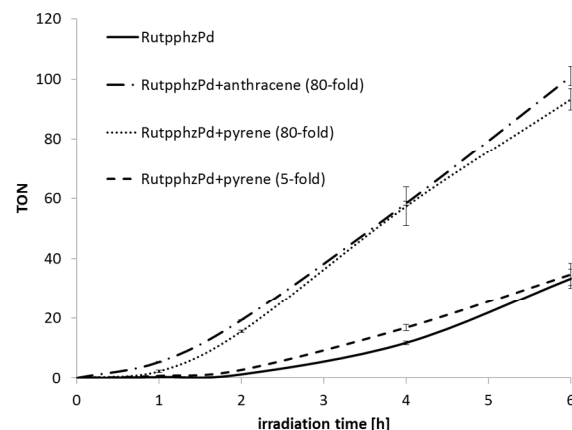


Fig. 7 Induction period of photocatalytic hydrogen production of **RutpphzPd** ($c = 70 \mu\text{M}$), **RutpphzPd** + anthracene (80-fold excess) and **RutpphzPd** + pyrene (80-fold and 5-fold excess) depending on the irradiation time; $\text{TON} = n(\text{H}_2)/n(\text{RutpphzPd})$. Error bars indicate the standard error of each value.

Especially the induction period, which lasts about 2 hours for **RutpphzPd** is shortened to less than 1 hour in the presence of a 80-fold excess of anthracene or pyrene. The addition of a 5-fold excess of pyrene leads to no significant changes in the catalytic behaviour. This effect would tentatively be explained by the relatively low degree of association of about 5% as determined previously. The addition of a 120-fold excess of pyrene shows no further improvement of the catalytic activity. This result suggests that the influence of pyrene within this area of degree of association (both about 50%) is nearly identical. Further, a time dependent catalytic behaviour can be observed. During the first 2 hours samples with anthracene and pyrene show a 10 fold increased activity. This increase is reduced at 4 hours to a factor of 5 and at 6 hours to a factor of 3. After 24 h no further increase in H_2 formation was observed for all samples and the final TON was identical within experimental errors (Table 4 and Table S1).

Table 4 TONs of **RutpphzPd**, * **RutpphzPd** with anthracene and **RutpphzPd** with pyrene after a certain time of LED light irradiation; values in brackets illustrate the standard deviation.

Irradiation time [h]	1	2	4	6
TON RutpphzPd + anthracene (80-fold)	5.3 (0.5)	19.3 (2.0)	58.4 (2.8)	100.9 (0.6)
TON RutpphzPd + pyrene (80-fold)	2.2 (0.6)	15.5 (0.6)	57.4 (9.2)	93.3 (5.0)
TON RutpphzPd + pyrene (120-fold)	2.9 (1.2)	13.8 (7.9)	44.4 (8.7)	88.6 (6.7)
TON RutpphzPd + pyrene (5-fold)	0.7 (0.1)	2.7 (0.1)	16.8 (1.1)	34.8 (3.6)
TON RutpphzPd	0.3 (0.2)	1.2 (0.1)	11.7 (0.8)	33.7 (4.5)

* final TON for all experiments was 190 ± 10

Both aromatic compounds, anthracene and pyrene show an almost identical effect on the catalytic activity of **RutpphzPd**, which is surprising considering the previously discussed photocatalytic dimerization of anthracene. As there is no $\pi\text{-}\pi$ -interaction possible between the anthracene dimer and **RutpphzPd**, one would expect a much less pronounced effect on the catalytic activity for anthracene compared to pyrene. To investigate this aspect in more detail, *in situ* UV/vis-spectroscopy was applied. Therefore a sample containing the photocatalyst **RutpphzPd** ($c = 3.5 \mu\text{M}$), anthracene (2.8 mM), water ($v\% = 0.5$) and TEA (0.1 M), was irradiated under exclusion of oxygen and the changes of the anthracene absorption in the range of $300\text{--}400 \text{ nm}$ were investigated.

Figure 8 shows that in the presence of TEA only a slight decrease of the anthracene related absorption bands was observed. Hence, the formation of the hydrogen evolving photocatalytically active **RutpphzPd** species must occur faster and more efficiently than the energy transfer from the excited ruthenium centre to the anthracene as this would lead to the formation of the anthracene dimer.

In order to investigate the photochemical interaction between **Rutpphz** and anthracene in solution in more detail Stern-Volmer analyses were performed. The emission quenching of **Rutpphz** by anthracene in acetonitrile could be analysed and yielded a dynamic Stern Volmer constant of $K_{SV} = 1000 \pm 14 \text{ M}^{-1}$ (see Supp. Info. Fig. S14). An interpretation of this observation is fundamentally limited, as we have no association Stern Volmer constant data from $^1\text{H-NMR}$ spectroscopy investigation. However, the fact that H_2 evolution is possible in the presence of anthracene despite this relatively high constant is another indication that the large excess of TEA in catalytic mixtures inhibits the dimerization of anthracene.

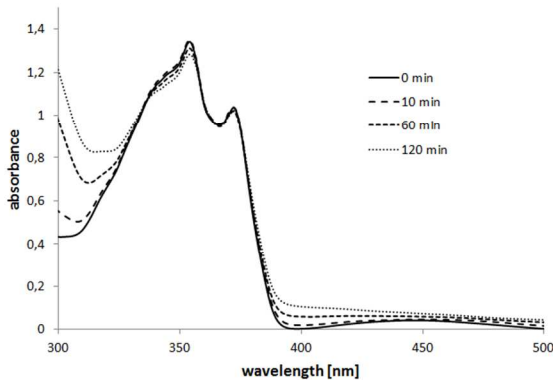


Fig. 8 Changes in the absorption spectrum of anthracene with **RutpphzPd** under catalytic conditions with TEA as electron donor ($c(\text{anthracene}) = 0.28 \text{ mM}$, $c(\text{RutpphzPd}) = 3.5 \mu\text{M}$, $c(\text{TEA}) = 0.1 \text{ M}$, $v\% (\text{H}_2\text{O}) = 0.5 \%$) with continuous LED light irradiation (470 nm).

A very tempting interpretation of the observed positive effects utilises the known light switch effect for ruthenium oligopyridophenazine complexes. As recently shown by x-ray structural analysis $\pi\text{-}\pi$ -interaction between the phenazine ligand and base pairs of the DNA protect the phenazine motive thus stabilising the luminescent states.^{47,48} We investigated therefore whether the interaction between pyrene and **RutpphzPd** shows positive steric effects, too. In the case of the structurally related

$\text{Ru}(\text{bpy})_2\text{dppz}^{2+}$ the addition of DNA leads to an intercalation of the planar dppz ligand into the DNA base pairs, which protects the phenazine moiety from hydrogen bond formation with water and so “switches on” the ruthenium centre based emission, which is otherwise quenched by water.^{49,50} To test whether a similar shielding effect can be observed for pyrene stacking on **RutpphzPd**, emission-quenching experiments were performed. Since the dinuclear **RutpphzPd** is non-emissive, the mononuclear **Rutpphz** was used as model compound instead. Therefore the emission intensities of probes containing **Rutpphz** ($c = 1 \mu\text{M}$) and pyrene ($c = 80 \mu\text{M}$) were compared to those additionally containing water ($c = 1.8 \text{ M}$). Surprisingly, the addition of pyrene had no positive effect on the emission quenching by water (see Supp. Info. Fig. S16). Hence, a DNA like protection of the phenazine unit as observed for $\text{Ru}(\text{bpy})_2\text{dppz}^{2+}$ is a rather unlikely explanation for the observed effects. Identical investigations with anthracene were not performed due to its dimerization.

Conclusions

Supramolecular $\pi\text{-}\pi$ -interaction is a dominant feature in the intermolecular interaction of tetrapyridophenazine ruthenium complexes as shown by solution based NMR and solid state X-ray investigations. Within this context we here present the first detailed investigation of solid state structure of **RutpphzPd**. It is possible to utilize this interaction for the formation of relatively stable one to one associates containing one planar polyaromatic partner, pyrene. Detailed investigations with anthracene as related organic partner have been precluded due to the fast photocatalytic dimerization of anthracene induced by the ruthenium complex. These results open a structural aspect as the formation of defined adducts based on a specific structural property is evident. Furthermore, a significant degree of photochemical interaction between the aromatic binding partner and the ruthenium complex is evident. In combination construction of advanced functional supramolecular architectures structurally based on carefully adjusted $\pi\text{-}\pi$ -interaction performing light driven reactions seems feasible.

The investigations on the effect of anthracene and pyrene addition on the photocatalytic activity of **RutpphzPd** yielded very similar results. In view of the observed photocatalytic dimerization taking place with anthracene, this similarity is a very surprising result. The addition of the 80-fold excess of the planar aromatic carbon species leads to a reduced induction period and increased turn over frequency during the initial phase of catalysis. The hypothetical explanation for this observation could be the supramolecular protection of the tpphz-ligand similar to the DNA induced light switch effect³⁴ by the polyaromatic carbon compounds. This could not be substantiated since the addition of water to a **Rutpphz**/pyrene mixture did lead to a significant loss of emission intensity. Another potential explanation could be brake up of **RutpphzPd** aggregates due to the interaction with the polyaromatic compounds resulting in a faster generation of the reactive species under photocatalytic conditions. At first sight the result for the anthracene effect on the photocatalytic behavior is puzzling but could be explained by *in situ* UV/vis spectroscopic investigations of the active catalytic system. Obviously is the photochemical reduction of the excited ruthenium complex

significantly faster than the energy transfer between the ruthenium centre and the anthracene. This aspect may open an indirect access to rate constants within active working photocatalysts. These constants are currently difficult to obtain due to the transient nature of any electronically excited state in active catalysts.

The results shown suggest that the activity of molecular photocatalysts can be tuned by carefully exploiting supramolecular effects. This area will require more in depth analysis in order to be fully exploited. The observed effects in connection with anthracene point towards caution with respect to transferring conclusions from model experiments into real catalytic reactions.

Acknowledgments

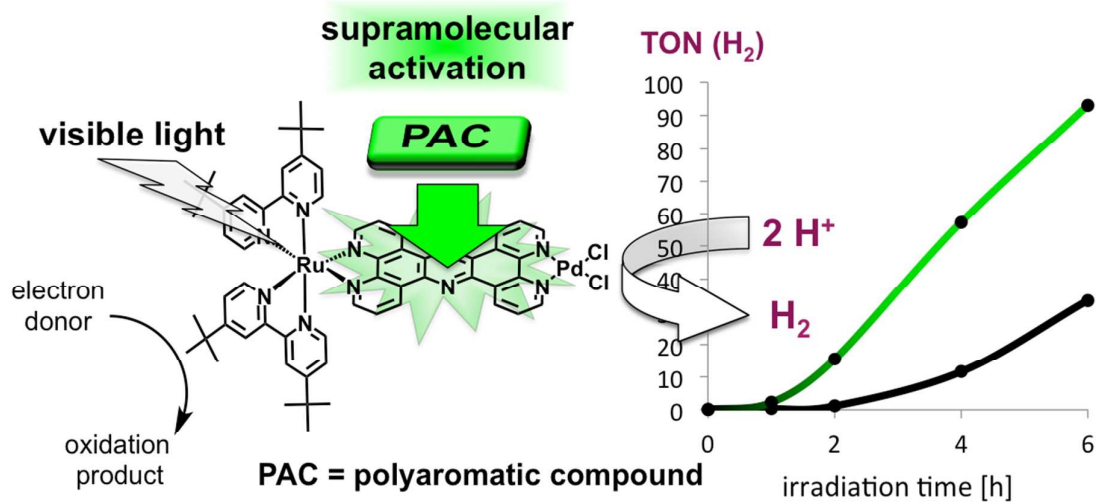
This research is supported by the German Research Association ((DFG SFB 583, DFG GRK 1626, MP and RS), the Deutsche Bundesstiftung Umwelt (DBU, CP), the Elitenetzwerk Bayern (RS), the Graduate School Molecular Science FAU Erlangen Nuremberg (RS) and the Carl-Zeiss-Stiftung (DS). Furthermore we thank Prof. Dr. G. Taubmann for his kind support.

Notes and references

- ^a University of Ulm, Institute of Inorganic Chemistry Materials and Catalysis, Albert-Einstein-Allee 11, 89081 Ulm. Fax: +49 731 5023039; Tel: +49 731 5023900; E-mail: sven.rau@uni-ulm.de.
- ^b Friedrich-Alexander-University of Erlangen-Nuremberg, Institute of Inorganic Chemistry, Egerlandstraße 1, 91058 Erlangen
- † Electronic Supplementary Information (ESI) available: [details of any supplementary information available should be included here]. See DOI: 10.1039/b000000x/
- 1 V. Balzani, Photochemical molecular devices, *Photochem. Photobiol. Sci.*, 2003, **2**, 459.
 - 2 C. Li, M. Wang, J. Pan, P. Zhang, R. Zhang and L. Sun, *J. Organomet. Chem.*, 2009, **694**, 2814.
 - 3 H. Ozawa, M. Haga and K. Sakai, *J. Am. Chem. Soc.*, 2006, **128**, 4926.
 - 4 A. Fihri, V. Artero, A. Pereira and M. Fontecave, *Dalton Trans.*, 2008, **41**, 5567.
 - 5 A. Fihri, V. Artero, M. Razavet, C. Baffert, W. Leibl and M. Fontecave, *Angew. Chem. Int. Ed.*, 2008, **47**, 564.
 - 6 M. Elvington, J. Brown, S. M. Arachchige and K. J. Brewer, *J. Am. Chem. Soc.*, 2007, **129**, 10644.
 - 7 S. Rau, B. Schäfer, D. Gleich, E. Anders, M. Rudolph, M. Friedrich, H. Görts, W. Henry and J. G. Vos, *Angew. Chem. Int. Ed.*, 2006, **45**, 6215.
 - 8 M. Karnahl, C. Kuhnt, F. W. Heinemann, M. Schmitt, S. Rau, J. Popp and B. Dietzek, *Chem. Phys.*, 2012, **393**, 65.
 - 9 F. Li, Y. Jiang, B. Zhang, F. Huang, Y. Gao and L. Sun, *Angew. Chem. Int. Ed.*, 2012, **51**, 2417.
 - 10 S. Sato, T. Morikawa, T. Kajino and O. Ishitani, *Angew. Chem. Int. Ed.*, 2013, **52**, 988.
 - 11 Y. Tamaki, T. Morimoto, K. Koike and O. Ishitani, *Proc. Natl. Acad. Sci. U.S.A.*, 2012, **109**, 15673.
 - 12 E. Amouyal, *Sol. Energy Mater. Sol. Cells*, 1995, **38**, 249.
 - 13 J.-M. Lehn and J.-P. Sauvage, *Nouv. J. Chim.*, 1977, **1**, 449.
 - 14 K. Kalyanasundaram, J. Kiwi, and M. Grätzel, *Helv. Chim. Acta*, 1978, **61**, 2720.
 - 15 M. Kirch, J.-M. Lehn and J.-P. Sauvage, *Helv. Chim. Acta*, 1979, **62**, 1345.
 - 16 S. Hansen, M. Klahn, T. Beweries and U. Rosenthal, *ChemSusChem*, 2012, **5**, 656.
 - 17 E. Amouyal, *Sol. Energy Mater. Sol. Cells*, 1995, **38**, 249.
 - 18 K. Maeda and K. Domen, *J. Phys. Chem. Lett.*, 2010, **1**, 2655.
 - 19 J. R. Bolton, *A review. Sol. Energy*, 1996, **57**, 37.
 - 20 Y. H. Hu, *Angew. Chem. Int. Ed.*, 2012, **51**, 12410.
 - 21 M. Karnahl, C. Kuhnt, F. Ma, A. Yartsev, M. Schmitt, B. Dietzek, S. Rau and J. Popp, *ChemPhysChem*, 2011, **12**, 2101.
 - 22 M. Karnahl, C. Kuhnt, F. W. Heinemann, M. Schmitt, S. Rau, J. Popp and B. Dietzek, *Chemical Physics*, 2012, **393**, 65.
 - 23 S. Losse, J. G. Vos and S. Rau, *Coord. Chem. Rev.*, 2010, **21-22**, 2492.
 - 24 S. Tschierlei, M. Presselt, C. Kuhnt, A. Yartsev, T. Pascher, V. Sundström, M. Karnahl, M. Schwalbe, B. Schäfer, S. Rau, M. Schmitt, B. Dietzek and J. Popp, *Chem. Eur. J.*, 2009, **15**, 7678.
 - 25 V. Artero, M. Chavarot-Kerlidou and Marc Fontecave, *Angew. Chem. Int. Ed.*, 2011, **50**, 7238.
 - 26 H. Ozawa, M. Kobayashi, B. Balan, S. Masaoka and K. Sakai, *Chem. Asian J.*, 2010, **5**, 1860.
 - 27 H. Ozawa and K. Sakai, *Chem. Commun.*, 2011, **47**, 2227.
 - 28 S. Tschierlei, M. Karnahl, M. Presselt, B. Dietzek, J. Guthmüller, L. González, M. Schmitt, S. Rau and J. Popp, *Angew. Chem. Int. Ed.*, 2010, **49**, 3981.
 - 29 S. D. Bergman and M. Kol, *Inorg. Chem.*, 2005, **44**, 1647.
 - 30 D. Gut, A. Rudi, J. Kopilov, I. Goldberg and M. Kol, *J. Am. Chem. Soc.*, 2002, **124**, 5449.
 - 31 S. D. Bergman, D. Reshef, S. Groysman, I. Goldberg and Moshe Kol, *Chem. Commun.*, 2002, 2374.
 - 32 S. D. Bergman, D. Reshef, L. Frish, Y. Cohen, I. Goldberg and Moshe Kol, *Inorg. Chem.*, 2004, **43**, 3792.
 - 33 S. D. Bergman, I. Goldberg, A. Barbieri and M. Kol, *Inorg. Chem.*, 2005, **44**, 2513.
 - 34 D. A. Lutterman, A. Chouai, Y. Liu, Y. Sun, C. D. Stewart, K. R. Dunbar and C. Turro, *J. Am. Chem. Soc.*, 2008, **130**, 1163.
 - 35 Y. Liu, A. Chouai, N. N. Degtyareva, D. A. Lutterman, K. R. Dunbar and C. Turro, *J. Am. Chem. Soc.*, 2005, **127**, 10796.
 - 36 S. Rau, B. Schäfer, D. Gleich, E. Anders, M. Rudolph, M. Friedrich, H. Görts, W. Henry and J. G. Vos, *Angew. Chem. Int. Ed.*, 2006, **45**, 6215.
 - 37 G.M. Sheldrick, *Acta Cryst.*, 2008, **A64**, 112.
 - 38 A.L. Spek, *J. Appl. Cryst.*, 2003, **36**, 7.
 - 39 A.L. Spek, *Acta Cryst.*, 2009, **D65**, 148.
 - 40 E. F. Wilson, H. Abbas, B. J. Duncombe, C. Streb, D.-L. Long, L. Cronin, *J. Am. Chem. Soc.* 2008, **130**, 13876.
 - 41 Ha, K. *Acta Cryst.* 2010, **E66**, m38.
 - 42 V. Steullet and D. W. Dixon, *Chem. Soc., Perkin Trans. 2*, 1999, 1547.
 - 43 N. R. de Tacconi, R. Chitakunye, F. M. MacDonnell and R. O. Lezna, *J. Phys. Chem. A*, 2008, **112**, 497.
 - 44 R. R. Islangulov and F. N. Castellano, *Angew. Chem. Int. Ed.*, 2006, **45**, 5957.
 - 45 L. Fielding, *Tetrahedron*, 2006, **56**, 6151.
 - 46 P. Thordarson, *Chem. Soc. Rev.*, 2011, **40**, 1305.
 - 47 H. Niyazi, J. P. Hall, K. O'Sullivan, G. Winter, T. Sorensen, J. M. Kelly, C. J. Cardin, *Nature Chemistry*, 2012, **4**, 621.
 - 48 J. P. Hall, D. Cook, S. R. Morte, P. McIntyre, K. Buchner, Hanna Beer, D. J. Cardin, J. A. Brazier, Graeme Winter, J. M. Kelly and C. J. Cardin, *J. Am. Chem. Soc.*, 2013, **135**, 12652-12659.
 - 49 M. Schwalbe, M. Karnahl, S. Tschierlei, U. Uhlemann, M. Schmitt, B. Dietzek, J. Popp, R. Groake, J. G. Vos and S. Rau, *Dalton Trans.*, 2010, **39**, 2768.
 - 50 Y. Sun, S. N. Collins, L. E. Joyce and C. Turro, *Inorg. Chem.*, 2010, **49**, 4257.

Supramolecular activation of a molecular photocatalyst

Michael G. Pfeffer, Christian Pehlken, Robert Staehle, Dieter Sorsche, Carsten Streb and Sven Rau*



Supramolecular activation of an intramolecular ruthenium palladium hydrogen evolving photocatalyst by polyaromatic compounds.